CONF-940222--14

ATTACK OF SUPERHEATER TUBE ALLOYS, COATINGS, AND CLADDINGS BY COAL-ASH CORROSION

S. Van Weele and J. L. Blough
Foster Wheeler Development Corporation
12 Peach Tree Hill Road
Livingston, NJ 07039

J. H. DeVan
Oak Ridge National Laboratory
Building 4500 S
Oak Ridge, TN 37831

ABSTRACT

Twenty stainless steels, nickel alloys, claddings, and intermetallics have been evaluated for their resistance to coal-ash attack. Six series of tests were conducted to determine the effects of two gas and three ash compositions at 650 and 700°C (1202 and 1292°F) for times up to 800 hours.

Keywords: Coal-ash corrosion, coal-fired boilers, alkali-iron trisulfate, stainless steels.

INTRODUCTION

Fireside corrosion has been a major cause of failure in the superheater region of pulverized-coal-fired boilers. This corrosion is caused by a liquid alkali-iron trisulfate (AIT) phase forming on the tube surface. The formation of this phase is primarily dependent upon three factors: temperature, SO_2 concentration in the flue gas, and alkali concentration in the coal ash.[1,2] Molten trisulfates can exist between 600 (1112) and 725°C (1337°F) (Figure 1). New boilers with steam temperatures above 538°C (1000°F) and older boilers with insulating steamside scales have tube O.D. skin temperatures in this range. This study evaluated potential alloys for use in superheaters of coal-fired boilers operating in a regime where liquid AIT can form.

EXPERIMENTAL PROCEDURE

The experimental setup and procedures used in this project are based upon previous studies by Rehn.[2] A testing cycle consisted of the following: Coupons were coated with synthetic coal ash, placed in a retort, and heated under a nitrogen purge to the exposure temperature, then exposed to simulated flue gas at this temperature for 100 hours. After exposure, the coupons were cooled under nitrogen. Before exposure, a fresh layer of ash was applied to the ash-covered coupons. Selected coupons were steam

cleaned and recoated to evaluate the effects of ash removal. Coupons were cycled in this manner up to eight times for a cumulative total exposure of 800 hours for each sample. Coupons were exposed to one of various conditions in this study: Three different ashes, two levels of SO_2, and two temperatures were evaluated.

Thicknesses of the unexposed specimens were measured by a flat micrometer, while the thicknesses of exposed specimens were measured using a point micrometer. Initial thickness readings were taken at each corner and in the middle of the specimens. After exposure, the average thickness loss was determined by again measuring the specimens at each corner and in the middle, and subtracting the average of the final measurements from the average of the initial measurements. The maximum thickness loss was determined by surveying the specimen to locate the thinnest area and subtracting its thickness from the average thickness of the unexposed specimen.

The ash compositions are listed in Table 1. Ash 1 was considered a "worst-case" composition, much more aggressive than typical service-derived coal ash. Ashes 2 and 3 are similar to those found in boilers burning high-sulfur Eastern subbituminous coal.

Coupons were exposed to gases similar to those in boilers burning medium- to high-sulfur coals. The gases contained 3.6% O_2, 14.0% CO_2, 10.0% H_2O, with 0.25% SO_2 for gases simulating the burning of a medium-sulfur coal or 1.0% SO_2 for gases simulating the burning of a high-sulfur coal. Nitrogen was the balance of the gas composition. In boilers, a portion of the SO_2 is catalyzed to SO_3. To create similar conditions in the laboratory, the gases were passed through iron turnings, which catalyze SO_3 formation, before they were passed over the coupons.

Chemical specifications of the exposed alloys and claddings are listed in Table 2. In addition, chromized/siliconized mild steel was tested; these coupons were supplied by The Ohio State University.[3]

EXPERIMENTAL RESULTS

Chromium content was found to be the largest factor in determining the resistance of an alloy to liquid AIT attack. Figure 2 is a compilation of sample thickness loss-rate data of all tests. For stainless steels and nickel alloys, additions of chromium up to 25% provide increased resistance to coal-ash attack; however, above the 25% chromium level, there does not appear to be any added benefit from more chromium. Silicon and aluminum were also beneficial, but to a lesser extent. The iron aluminide intermetallics also show a chromium dependence. Aluminides containing 5% chromium performed markedly better overall than those containing 2% chromium.

Four environmental parameters were examined in this study: time, temperature, ash composition, and concentration of SO_2 in the flue gas. Additionally, the effects of cleaning the preexisting ash layer off the coupon and redepositing a fresh ash between exposure cycles was evaluated (typical of soot blowing).

Corrosion rates for alloys in a moderately corrosive environment are shown in Figure 3 (arranged from left to right in order of increasing chromium level). The more resistant alloys show lower corrosion rates at longer exposure times, indicating the formation of a passive layer; the less-resistant alloys exhibit increasing corrosion rates at longer exposures. A seeming exception to this trend is CR35A. This alloy was very resistant to attack at 100 hours, indicating it may still be within the incubation period for attack in this environment.

Average thickness loss rates for a selection of alloys exposed at 650 (1202) and 700°C (1292°F) are shown in Figure 4. Lower-chromium alloys generally suffered greater wastage rates at the higher testing temperature [700°C (1292°F)], while higher-chromium alloys suffered the same amount of wastage at 650 (1202) as at 700°C (1292°F). Note that the corrosion rates of the alloys drop as the chromium content increases, illustrating the beneficial effect of chromium. The exception is the reduced corrosion rate of the 5% chromium in the iron-aluminide matrix.

Both the alkali content in the ash and SO_2 concentration in the flue gas affect the corrosivity of the alkali-iron trisulfates in the ash layer. As Figures 5 and 6 show, an increase in either results in a more corrosive environment and higher wastage rates.

The specimens that had the preexisting ash layer removed between cycles suffered slightly less attack than those that had fresh ash added atop the older ash layer (Figure 7). The corrosion rates of specimens cleaned between cycles may be lower because an induction period is needed for the alkali-iron trisulfate to reform. Specimens with an intact ash layer would be exposed to molten trisulfates as soon as they reached temperature.

MORPHOLOGY OF SPECIMENS

A photomacrograph of selected specimens is shown in Figure 8. These specimens exhibit the range of corrosion morphologies found during testing. The less resistant alloys, such as modified 316, exhibited uniform corrosion in all environments. More resistant alloys (690 for example) did not display any corrosion in the less aggressive environments. In the more aggressive environments, attack on these alloys took the form of trench-like pits between sections completely free from attack. The corrosion morphology on aluminides consisted of uneven, roughened patches which appeared to be influenced by the rolling texture on the specimens.

A 17-14 CuMo specimen coated with ash containing 10% alkali sulfates and exposed at 700°C (1292°F) in 1.0% SO_2 is shown in Figures 9 and 10. The interface between the metal and ash is smooth, with no indications of subsurface enrichment/depletion, intergranular attack, or the formation of subsurface sulfides and oxides. The maps of chemical concentration in Figure 10 confirm this by not showing any depletion or enrichment of the primary alloying elements or subsurface concentrations of sulfur. Regions of high sulfur and nickel or chromium in the ash layer may be pockets of chromium and nickel sulfide which have precipitated. The chromium level in this alloy was apparently too low to form a protective barrier against molten AIT, and the alloy was simply fluxed away with no subsurface interactions.

Figures 11 and 12 show a cross section of RA85H coated with ash after exposure for 200 hours at 700°C (1292°F). As shown in Figure 11, the surface is jagged, with evidence of intergranular attack and subsurface penetration. Chromium has been enriched along grain boundaries and at the interface, where it formed sulfides and oxides. Near the interface, where chromium depletion has taken place, nickel has been selectively enriched. The high concentration of sulfur at the interface, combined with areas that appear to be chromium and nickel sulfides, raises the possibility that oxidation-sulfidation reactions are taking place in addition to fluxing by molten AIT. Figure 13 displays an RA85H specimen which has been exposed for 800 hours at 700°C (1292°F). As shown in Figures 12 and 13, intergranular attack has taken place to a point where grains are beginning to fall out.

The corroded surface of a monolithic 690 specimen after exposure at 700°C (1292°F) is shown in Figures 14 and 15, with an accompanying x-ray map of chemical composition shown in Figure 16. As illustrated in both the optical photomicrograph and SEM image, the specimen is being attacked by a sulfidation and oxidation front moving down from the surface, depleting the surface metal of chromium. This depletion destroys the passive chromium oxide scale and allows AIT attack to occur. This form of attack is only noticeable in higher-alloy specimens exposed for longer than 100 hours.

For comparison with the laboratory specimens, an Alloy 310 Nb tube, which was exposed for 16,000 hours at the Tennessee Valley Authority's Gallatin Station, is shown in Figures 17 and 18.[4] The corrosive attack on this specimen is fully developed and may be assumed to have reached steady-state conditions. As illustrated in Figure 18, four attack mechanisms are occurring: Chromium has been depleted from the area around the grain boundaries, subsurface metal has been depleted of chromium and enriched in nickel, chromium sulfides have formed in the subsurface metal, and AIT attack has occurred. All of these attack mechanisms are found on various specimens exposed during laboratory testing, indicating that exposures conducted under laboratory conditions provide similar conditions to those found in operating utility boilers.

A pit in iron aluminide, filled with corrosion products, is shown in Figure 19, with an accompanying x-ray map of the metal and deposit shown in Figure 20. The deposit consists of a thin, sulfur-rich layer, surrounding a layer rich in iron. There appears to be no depletion in the alloy itself, in contrast to the stainless steels and nickel-based alloys. Rather, the corrosion front appears as a sharp demarcation between corroded material and sound alloy.

DISCUSSION AND CONCLUSIONS

A wide range of alloys has been evaluated in environments similar to those found in pulverized-coal-fired boiler superheaters. The predominant form of attack is coal-ash corrosion, which is caused by a liquid alkali-iron trisulfate layer forming next to the metal surface. Six series of tests were conducted to determine the effects of various environmental variables on the wastage rates of the alloys. The environmental factors that promote attack are a high level of alkalies in the ash, a high concentration of SO_2 in the flue gas, and a long exposure time with an undisturbed ash layer. Lower-chromium alloys had greater wastage rates at the higher testing temperature [700°C (1292°F)], while alloys with a higher chromium content had about the same wastage rates at both temperatures. Chromium was found to be the principal factor determining alloy resistance to attack under all conditions. The final report describing the complete research program has been published.[5]

By comparing corrosion morphologies, several trends are evident. Alloys with little intrinsic resistance to attack, or alloys exposed to highly aggressive environments, do not show subsurface penetration or chromium depletion. Instead, corrosion occurs by the alloy fluxing into the molten AlT. Alloys that were more resistant to attack in moderately aggressive environments suffered subsurface chromium depletion below the attacked areas. Alloy 310 Nb, which was exposed in an operating utility boiler, also exhibited subsurface chromium depletion, indicating that this is not an artifact created only by laboratory testing. Intergranular attack also occurs to varying degrees along with generalized subsurface attack on the more highly resistant alloys. A fully developed example of this attack can be seen on Alloy 310 Nb, which has been exposed for 16,000 hours.

REFERENCES

1. I. M. Rehn, "Laboratory Fireside Corrosion Evaluation of Improved Superheater Tube Alloys and Coatings," EPRI CS-3134, Project 6441, Final Report, June 1983.

2. J. L. Blough and S. Kihara, "Coal-Ash Corrosion in Superheater and Reheaters," Corrosion/88, paper no. 129 (Houston, TX: NACE, 1988).

3. M. A. Harper and R. A. Rapp, "Chromized/Siliconized Pack Cementation Diffusion Coatings for Heat Resistant Alloys," First International Conference on Heat-Resistant Materials, ASM International, Fontana, WI, 1991.

4. J. Blough, G. Stanko, and M. Krawchuk, "In-Situ Coal-Ash Corrosion Testing for 2 Years at Three Utilities," presented at the EPRI/Potomac Electric Power Co. International Symposium on Improved Technology for Fossil Power Plants--New and Retrofit Applications, Washington, DC, March 1-3, 1993.

5. S. Van Weele, "Fireside Corrosion Testing of Candidate Superheater Tube Alloys, Coatings, and Claddings," prepared for Oak Ridge National Laboratory under Contract DE-AC05-840R21400, August 1991.

TABLE 1
ASH COMPOSITIONS (wt%)

Ash 1	Ash 2	Ash 3
25 Fe_2O_3	90 Fe_2O_3	30 Fe_2O_3
37.5 Na_2SO_4	5 Na_2SO_4	5 Na_2SO_4
37.5 K_2SO_4	5 K_2SO_4	5 K_2SO_4
		30 Al_2O_3
		30 SiO_2

TABLE 2
COMPOSITION OF ALLOYS EXAMINED

Alloy	Fe	Ni	Cr	Mo	C	Si	Mn	Al	N	S	P	Other
Fe_3Al-2Cr	81.86		2.19					15.93				B 0.01
Fe_3Al-5Cr	77.5		5.6					15.9				
$(FeNi)_3Al$	11.7	70.1	7.2					11.0				
Modified 316	Bal	16.83	14.27	2.25	0.079	0.23	1.77	0.06	0.012	0.01	0.037	V 0.52, Nb 0.1, Ti 0.21
17-14 CuMo	Bal	14.08	16.37	1.95	0.078	0.72	0.88			0.005	0.023	Cu 3.34
Type 347*†	Bal	10.3	17.5		0.08	1.3	1.6			0.03	0.045	Nb 0.8
RA85H	Bal	15.26	18.50	0.06	0.24	3.90	0.50	0.70	0.10		0.015	Cu 0.39
Modified 800H	Bal	31.08	20.87	2.01	0.097	0.21	1.93	0.02	0.01	0.013	0.003	Nb 0.19, Ti 0.29, V 0.47
NF709*†	Bal	24.3	21.5	1.0-2.0	<0.2	0.7	<1.5		0.05-0.02	<0.01	<0.03	Nb 0.1 - 0.4
Haynes 556	Bal	22.1	21.55	2.83	0.1	0.4	0.95	0.13	0.16	0.002	0.006	Ta 0.68, Nb 0.07, W 2.45, B 0.01
HR3C†	Bal	20.45	24.95		0.06	0.42	1.28		0.23	0.001	0.013	Nb 0.45
690/316	9.09	57.3	31.65	<0.05	0.048	0.26	0.17			0.002	<0.005	
690/800H	9.13	57.3	31.50	<0.05	0.049	0.26	0.17			0.002	<0.005	
690*	9.5	Bal	30.0		0.03							
CR35A†	17.7	43.8	37.3				0.2					
72 Clad Lean Stainless Steel‡	0.27	55.89	43.73		0.01	0.07	0.03			0.001		
72 Clad 800H	0.55	55.3	43.00	0.067	0.041	0.15	0.025			0.001	0.006	
671 Clad Lean Stainless Steel‡		Bal	48.5	<0.05	0.057	0.11	<0.10	<0.05	0.0095	0.003	0.002	Ti 0.46, Nb <0.05, Cu <0.05
671*		Bal	48.0		0.05							Ti 0.35
Sandvik 28†	Bal	31.19	26.94	3.36	0.011	0.15	0.67		0.045	0.003	0.014	Cu 1.00

*Typical. †Supplied by FWDC, all others supplied by ORNL. ‡Modified Type 316.

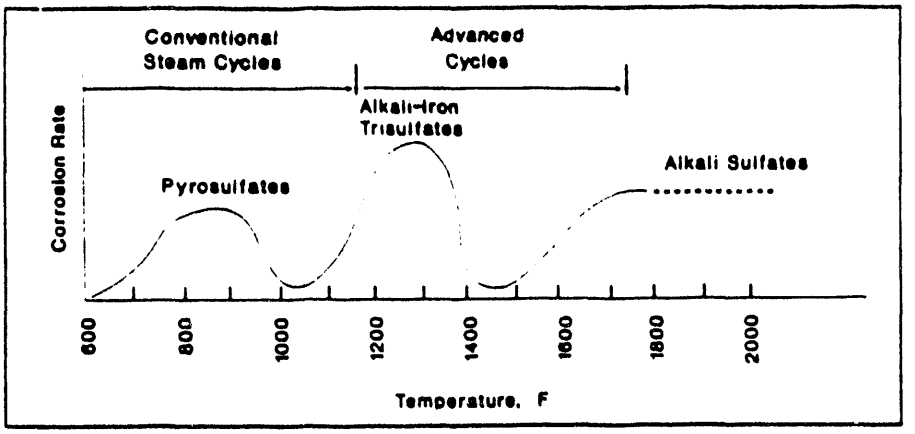

FIGURE 1 - Corrosion from alkali-sulfur compounds

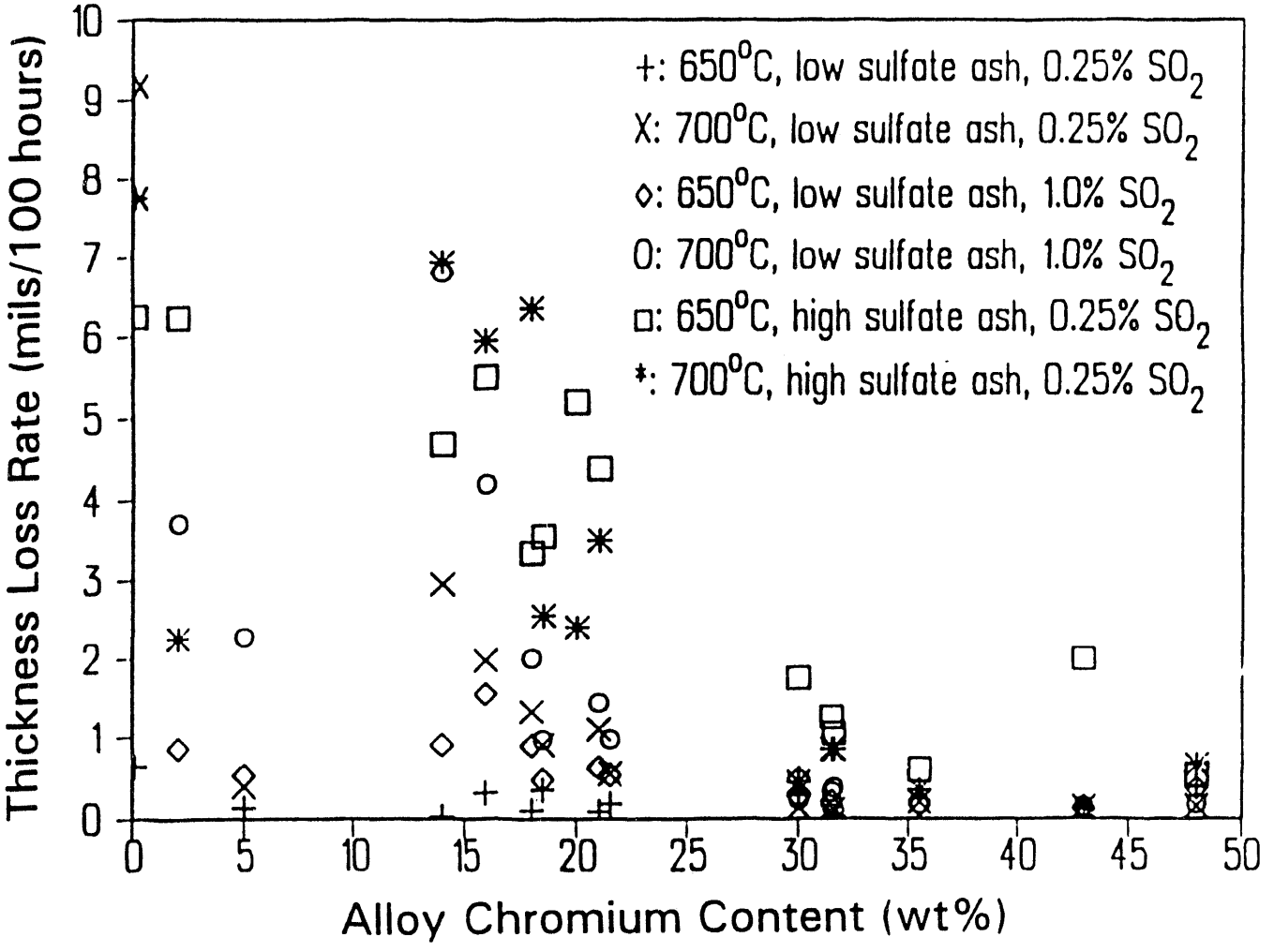

FIGURE 2 - Average thickness loss rate of alloy compared with chromium content of alloy (plot contains data for all alloys exposed under every environment tested in program)

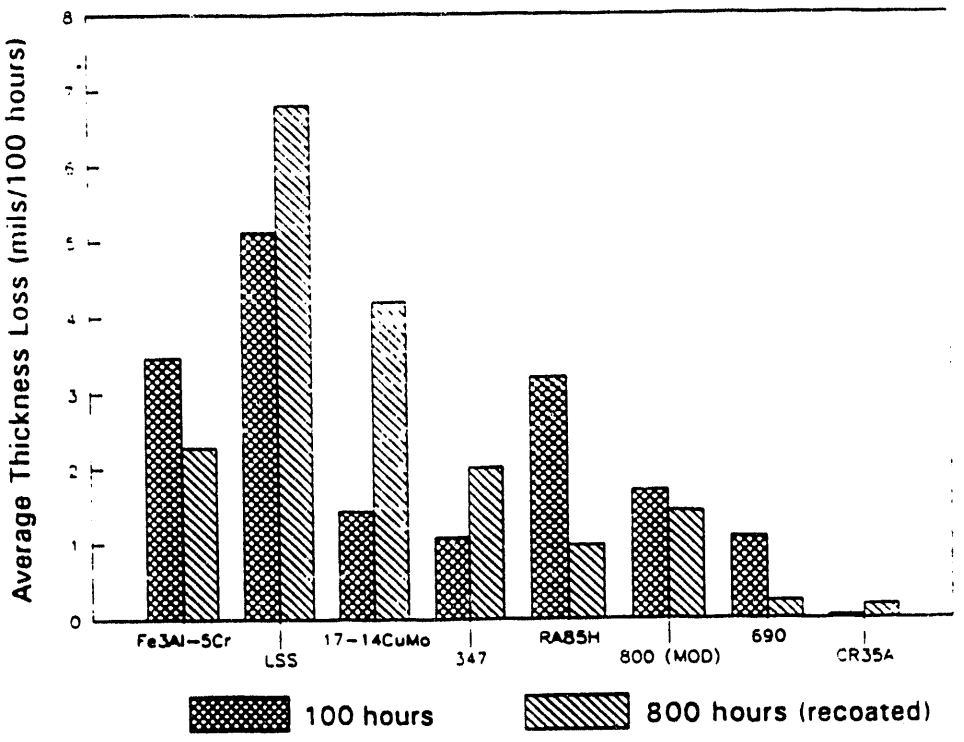

FIGURE 3 - Average thickness loss rates of representative alloys coated with ash containing 10 wt% alkali sulfates and exposed at 700°C (1292°F) for either 100 or 800 hours to flue gas containing 1.0 vol% SO_2

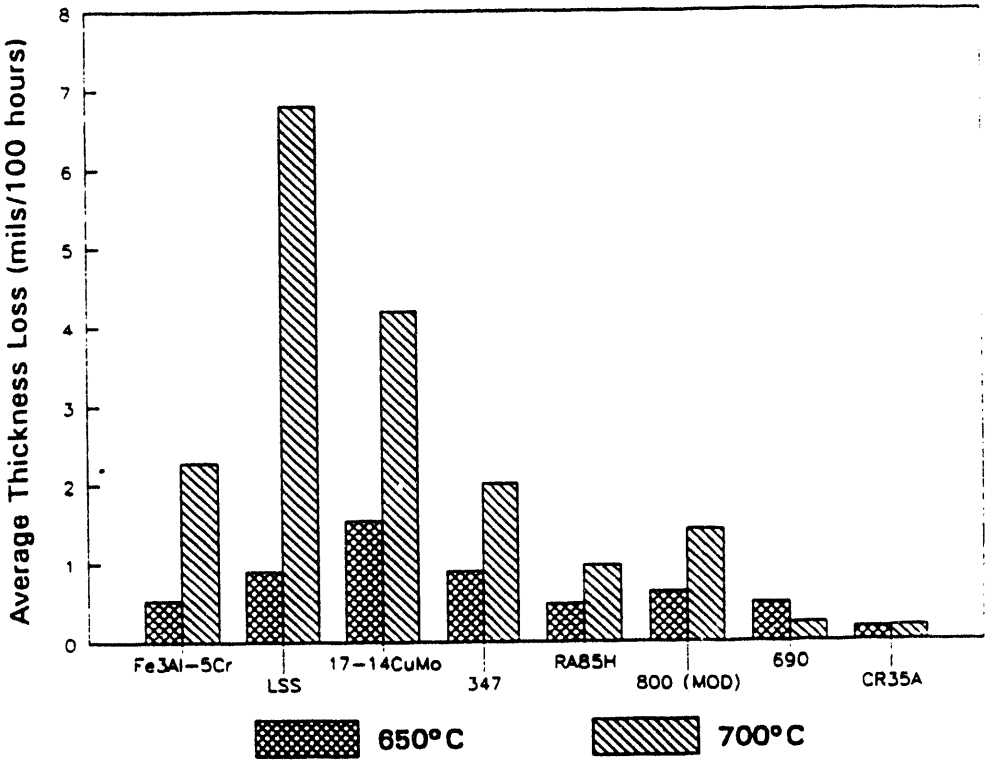

FIGURE 4 - Average thickness loss rates of representative alloys coated with ash containing 10 wt% alkali sulfates and exposed at 650 (1202) and 700°C (1292°F) for 800 hours to flue gas containing 1.0 vol% SO_2

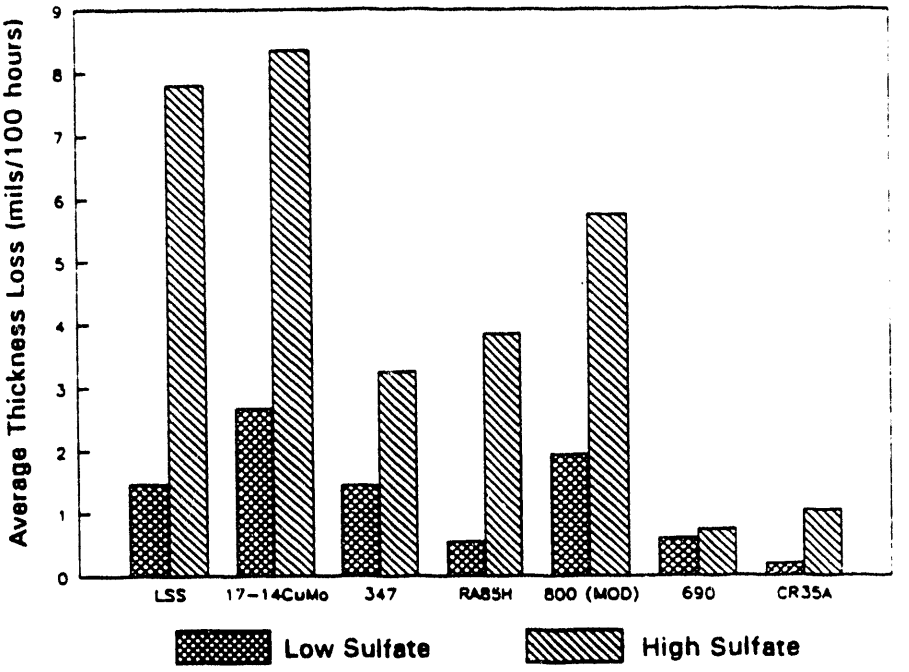

FIGURE 5 - Average thickness loss rates of representative alloys coated with ash containing either 10 or 75 wt% alkali sulfates and exposed at 700°C (1292°F) for 200 or 800 hours respectively to flue gas containing 0.25 vol% SO_2

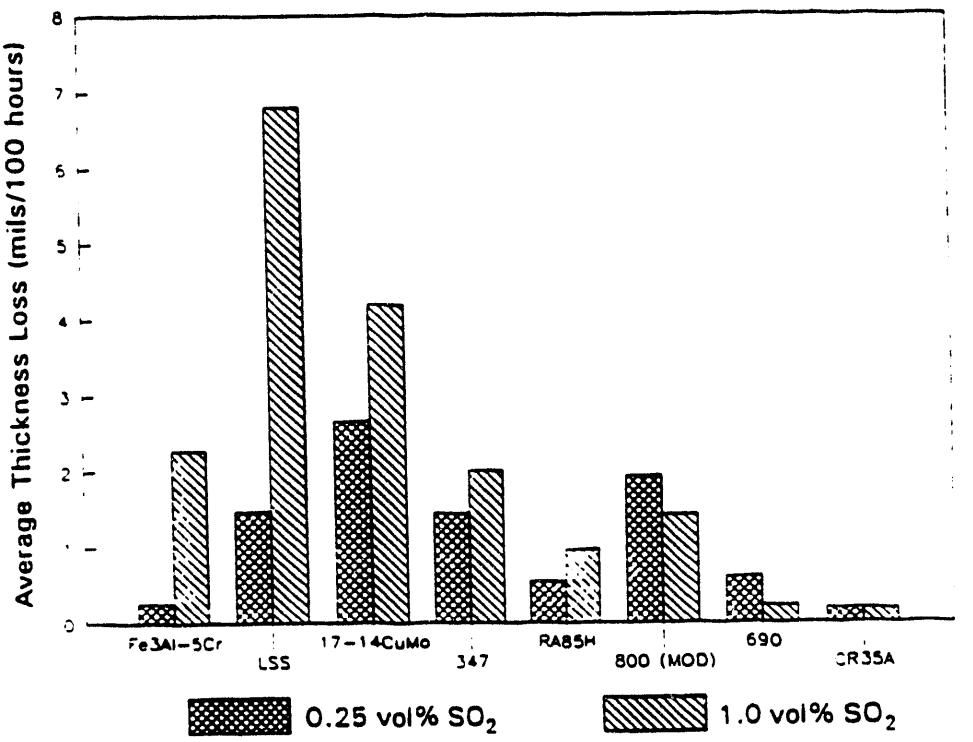

FIGURE 6 - Average thickness loss rates of representative alloys coated with ash containing 10 wt% alkali sulfates and exposed at 700°C (1292°F) for 800 hours to flue gas containing either 0.25 or 1.0 vol% SO_2

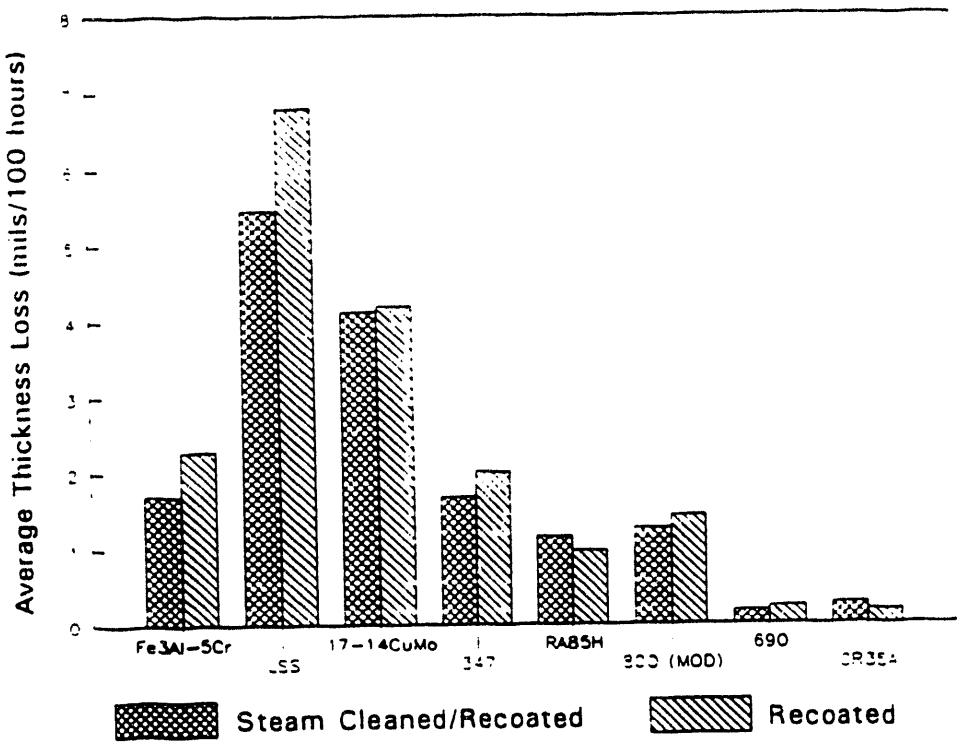

FIGURE 7 - Average thickness loss rates of representative alloys coated with ash containing 10 wt% alkali sulfates and exposed at 700°C (1292°F) for 800 hours to flue gas containing 1.0 vol% SO_2

16.6μ SEM Image

FIGURE 9 - Corroded surface of a 17-14 CuMo specimen coated with ash containing 10 wt% alkali sulfates after exposure for 200 hours at 700°C (1292°F) to flue gas containing 1.0 vol% SO_2. (Top area of image shows ash coating; bottom area is specimen.)

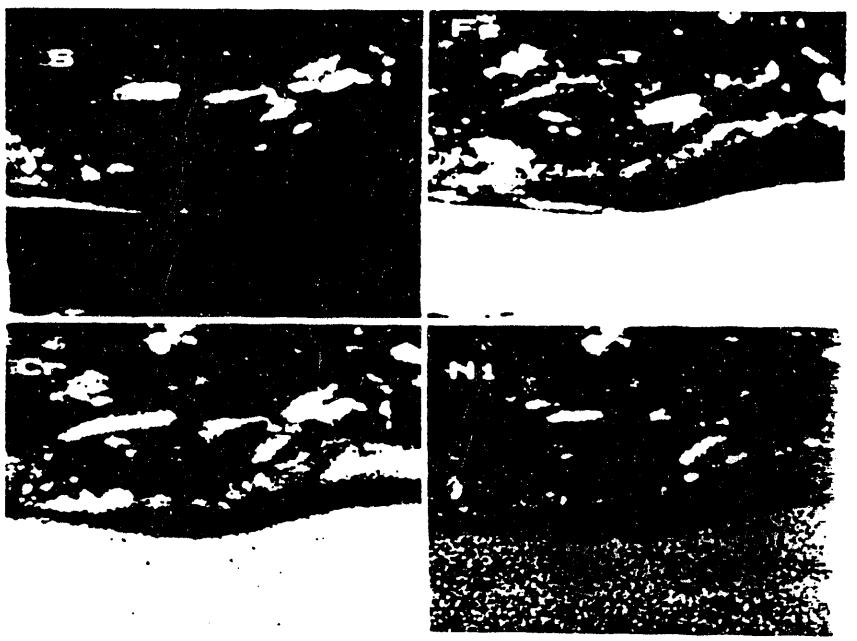

16.6μ Relative Concentration of Element

FIGURE 10 - X-ray map of corroded surface of a 17-14 CuMo specimen coated with ash containing 10 wt% alkali sulfates after exposure for 200 hours at 700°C (1292°F) to flue gas containing 1.0 vol% SO_2.

16.6μ

SEM Image

FIGURE 11 - Corroded surface of RA85H specimen coated with ash containing 10 wt% alkali sulfates after exposure for 200 hours at 700°C (1292°F) to flue gas containing 1.0 vol% SO_2. (Top area of image shows ash coating; bottom area is specimen.)

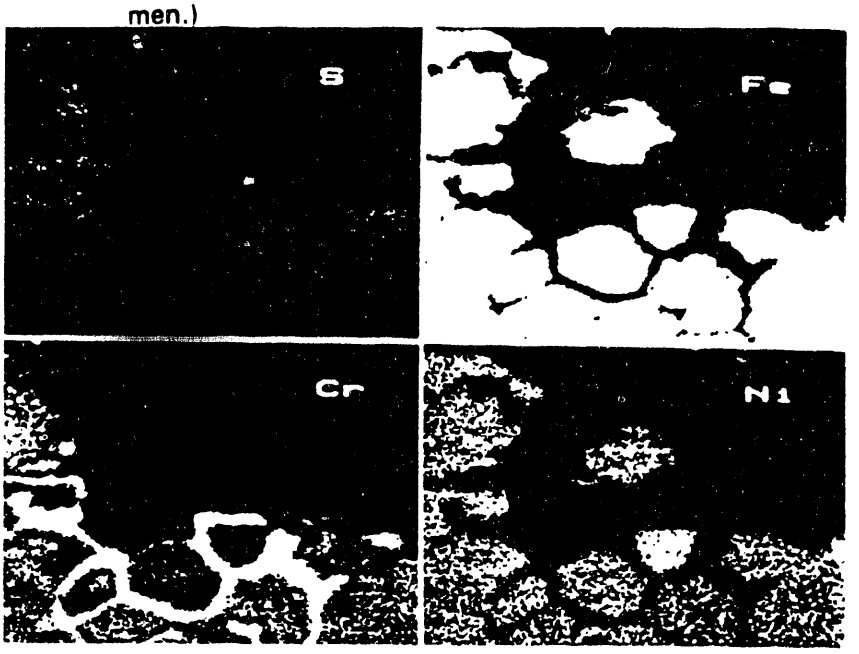

16.6μ

Relative Concentration of Element

FIGURE 12 - X-ray map of corroded surface of RA85H specimen coated with ash containing 10 wt% alkali sulfates after exposure for 200 hours at 700°C (1292°F) to flue gas containing 1.0 vol% SO_2

20μ

Oxalic Acid Etch

FIGURE 13 - Corroded surface of RA85H specimen coated with ash containing 10 wt% alkali sulfates after exposure for 800 hours at 700°C (1292°F) to flue gas containing 1.0 vol% SO_2. (Note intergranular attack on specimen surface.)

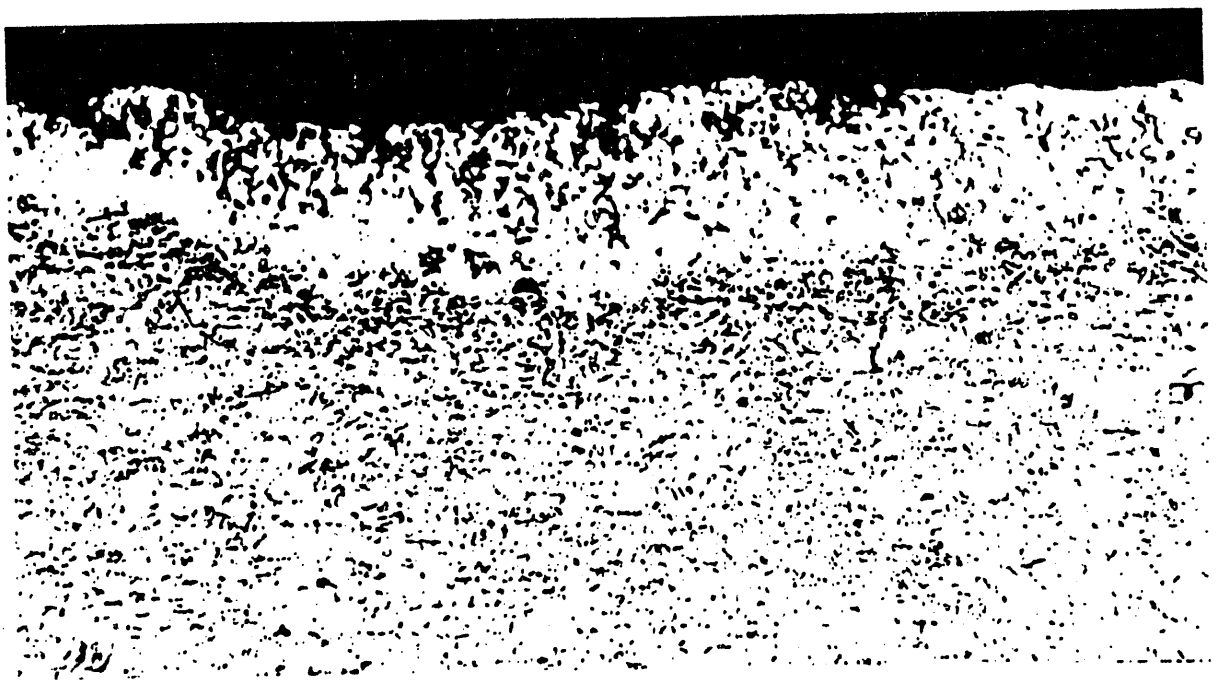

FIGURE 14 - Corroded surface of 690 specimen coated with ash containing 10 wt% alkali sulfates after exposure for 800 hours at 700°C (1292°F) to flue gas containing 1.0 vol% SO_2. (Note oxidation/sulfidation on specimen surface.)

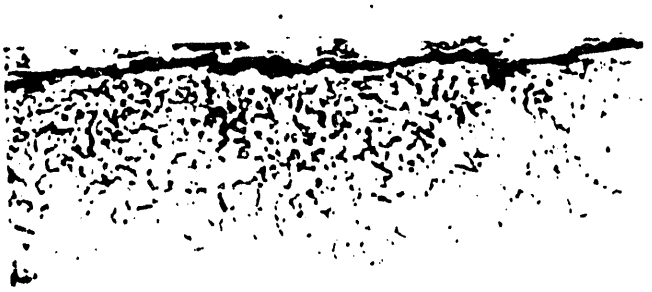

16.6μ

SEM Image

FIGURE 15 - Corroded surface of 690 specimen coated with ash containing 10 wt% alkali sulfates after exposure for 800 hours at 700°C (1292°F) to flue gas containing 1.0 vol% SO_2. (Note oxidation/ sulfidation on specimen surface.)

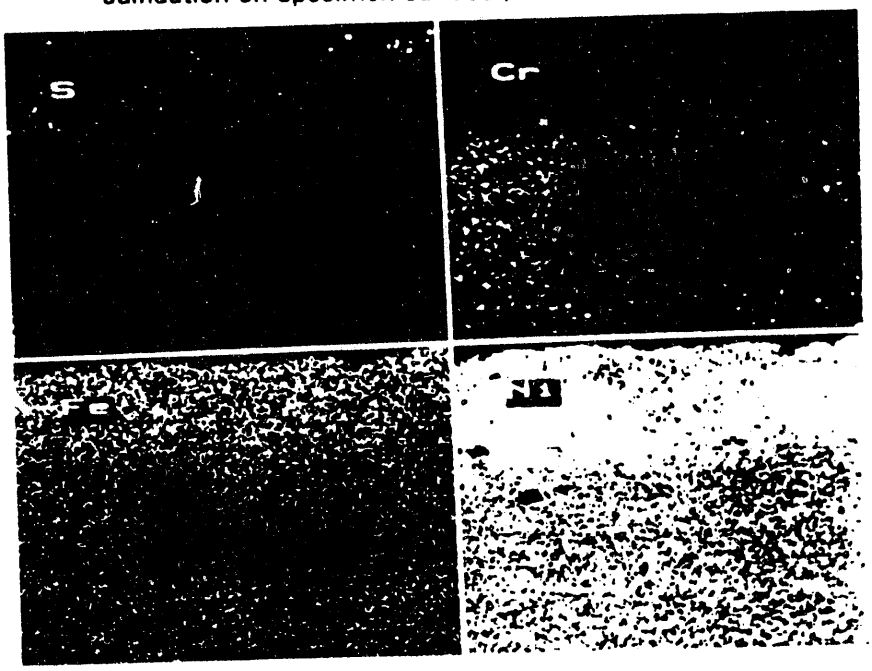

16.6μ

Relative Concentration of Element

FIGURE 16 - X-ray map of corroded surface of 690 specimen coated with ash containing 10 wt% alkali sulfates after exposure for 200 hours at 700°C (1292°F) to flue gas containing 1.0 vol% SO_2

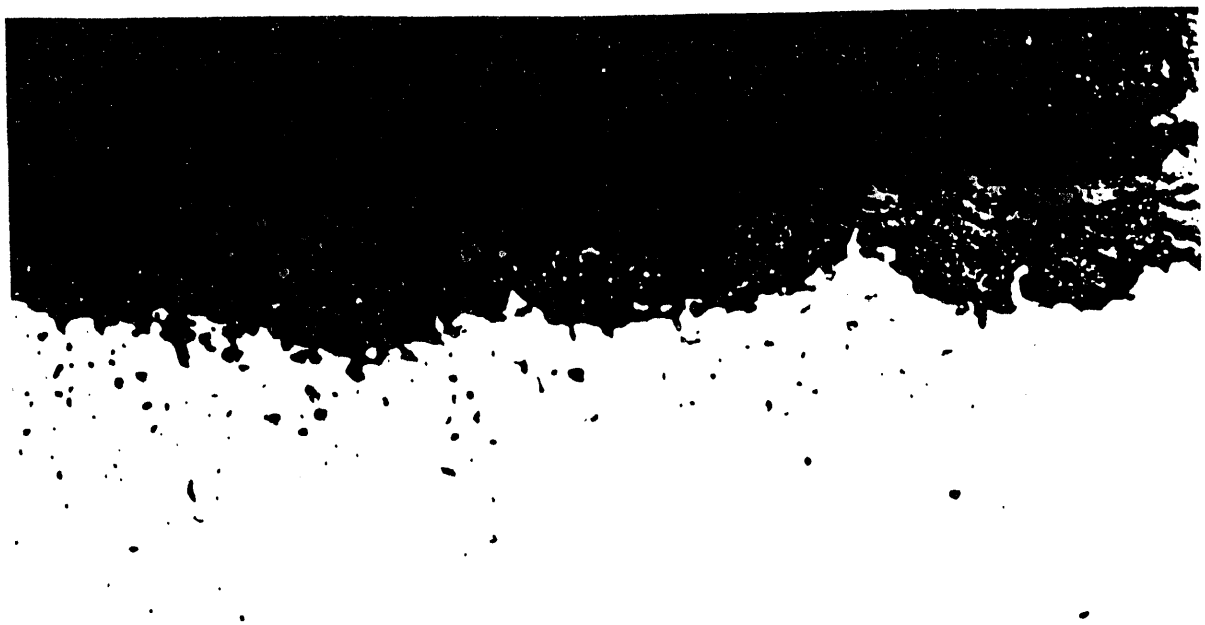

20μ

Unetched

FIGURE 17 - Corroded surface of 310 Nb after exposure in pulverized coal-fired boiler for 16,000 hours. (Note general sulfidation/oxidation below layer of scale.)

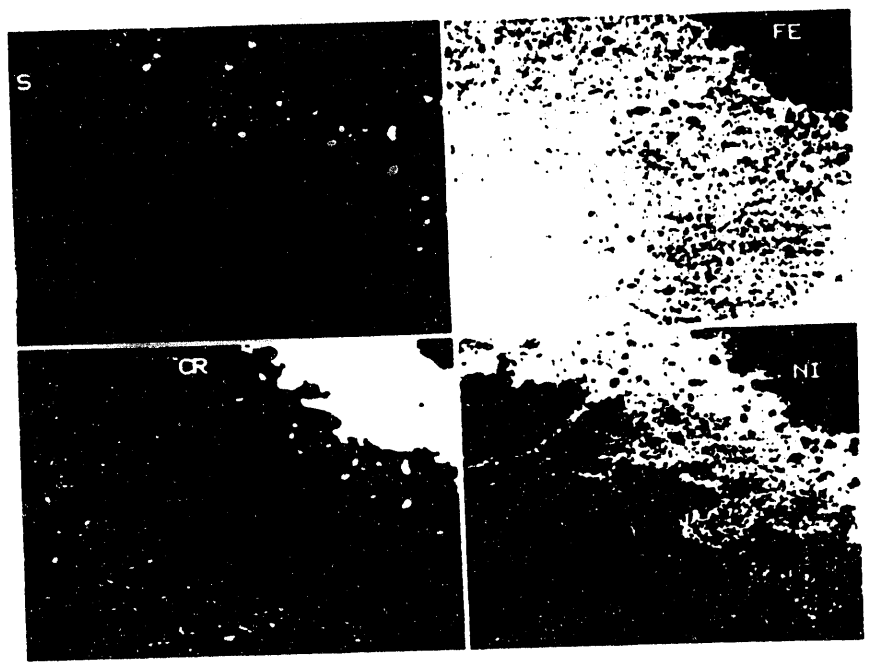

16.6μ

Relative Concentration of Element

FIGURE 18 - X-ray map of corroded surface of 310 Nb specimen after exposure for 16,000 hours in pulverized-coal-fired boiler

16.6μ

SEM Image

FIGURE 19 - Corroded surface of iron aluminide specimen containing 2% chromium coated with an ash containing 10 wt% alkali sulfates after exposure for 200 hours at 700°C (1292°F) to flue gas containing 1.0 vol% SO_2. (Note pit growing from specimen surface at bottom of photograph.)

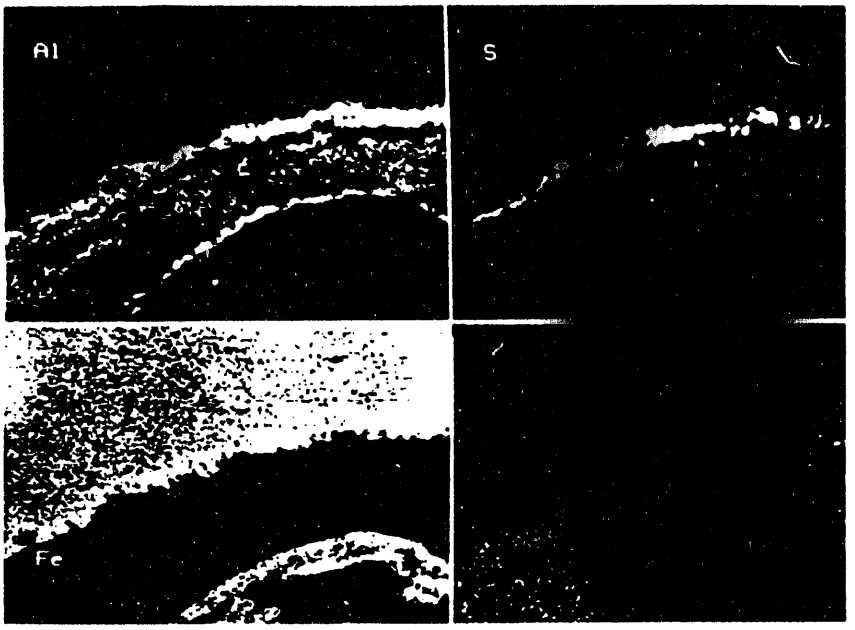

16.6μ

Relative Concentration of Element

FIGURE 20 - X-ray map of corroded surface of iron aluminide specimen containing 2% chromium coated with an ash containing 10 wt% alkali sulfates after exposure for 200 hours at 700°C (1292°F) to flue gas containing 1.0 vol% SO_2

ACKNOWLEDGMENTS

This research was sponsored by the Fossil Energy Advanced Research and Technology Development (AR&TD) Materials Program, U. S. Department of Energy, under contract DE-AC05-84OR21400 with Martin Marietta Energy Systems, Inc.

DISCLAIMER

DATE
FILMED
5/12/94
END